EX-SITU METHOD FOR FABRICATION OF NANOCOMPOSITE THICK-FILMS BASED ON MAGNETITE

Georgiana DOLETE[1], Denisa FICAI[2], Anton FICAI[1], Alexandra-Cătălina BÎRCĂ[1], Ludmila MOTELICA[1], Roxana TRUȘCĂ[1], Ovidiu Cristian OPREA[2], Marin GHEORGHE[3], Ecaterina ANDRONESCU[1]

In this study, we fabricated magnetic nanocomposite thick-films by an ex-situ method. Fabrication process involved synthesis of Fe_3O_4, and citrate coated Fe_3O_4, mixing the nanoparticles in a PDMS polymeric solution at 1:1 mass ratio and subsequently casting the composite material and applying a thermal treatment to achieve the final thick-films. The obtained nanoparticles were first characterized to confirm the formation of single-phase magnetite and the successful coating with citrate as well as to examine their morphology and magnetic behavior. We investigated the effects that both types of nanoparticles had on the homogeneity of the films, as well as the magnetic behavior of the films for potential further applications in drug delivery systems. The obtained films proved to be homogenous for both types of nanoparticles. Anyway, uncoated Fe_3O_4 in the PDMS matrix demonstrated better magnetic properties compared to coated Fe_3O_4.

Keywords: magnetic thick-film, nanocomposites, drug delivery systems, electromagnetic actuation

1. Introduction

With the development of first microelectromechanical system (MEMS), used as an insulin delivery system in the 1980s [1], micropumps became a common point of interest due to various applications they could satisfy in the field of microfluidics. Among the advantages of using such micropump, the most important that we can specify are the high versatility and potential of uses, it reduces the quantities of used sample/reagents, as well as time of analysis [2,3].

Over time, different types of actuating mechanisms had been developed like electrical, magnetic, thermal, optical and mechanical [1,3]. Lately, research has been focusing on electromagnetic actuation mechanisms. The most significant mechanism in electromagnetic actuation is a flexible structure that interacts with a magnetic component. Moving structures should be built of flexible material that can vibrate constantly and respond to mechanical pressure and magnetic fields [4].

[1] Depart. of Science and Engineering of Oxide Materials and Nanomaterials, University POLITEHNICA of Bucharest, Romania, e-mail: dolete.georgiana@gmail.com
[2] Depart. of Inorganic Chemistry Physical Chemistry and Electrochemistry, University POLITEHNICA of Bucharest, Romania
[3] SC NANOMEMS SRL, Brasov, Romania

The primary benefits of electromagnetic actuation are the strong magnetic force produced, which permits significant membrane deflection, and the high frequency tuning capacity. In addition, rapid electromagnetic field creation permits membrane deformation in two directions with a very quick vibration rate [5].

Several approaches for electromagnetic (EM) actuators have mainly focused on using permanent magnets attached to a polymeric membrane. For example, Yunas *et al.* [6] fabricated a 20 μm silicon-based membrane to which they attached a NdFeB magnet which was capable to deform the membrane up to 4.5 μm. Another study showed a magnet attached to a PDMS membrane and showed even higher displacements of approximately 100 μm [7]. Use of nanocomposite materials based on Fe_3O_4 have not been thoroughly explore, even though the materials show a great potential in obtaining functional electromechanical micropump, being capable of membrane displacements up to 33 μm [8]. Due to Fe_3O_4 biocompatibility, these types of micropumps could be used for implantable devices.

Chemical methods for synthesizing magnetic nanoparticles proved to be effective methods for achieving uniform particles with small size distribution. Among the chemical methods, co-precipitation in alkaline aqueous solution showed to be the most simple and common route for synthesis of magnetite nanoparticles (Fe_3O_4 NPs), even at high productivity [9,10]. Typically, magnetic nanoparticles are coated with various organic or inorganic molecules [11] that offer them colloidal stability and make them more water dispersible [12]. A proper coating of the magnetic nanoparticles reduces risks of dissolution *in vivo*, agglomeration or precipitation, which can be very important for biomedical applications.

In conclusion, we aimed in obtaining a nanocomposite magnetic thick-films which offers great potential in using them as components for magnetically actuated micropumps. The study had been oriented towards fabrication and physico-chemical characterization of the magnetic film.

2. Materials and methods

All chemicals used were analytical grade and purchased from Sigma-Aldrich, USA.

2.1. Fe_3O_4 and coated-Fe_3O_4 synthesis

Fe_3O_4 nanoparticles were obtained by co-precipitation. Equal volumes of solutions of a mixture of bivalent and trivalent iron salts in a molar ratio of 1:2 was added dropwise over a NaOH solution. Initially, 10 g of sodium hydroxide is dissolved in 250 ml of distilled water under vigorous mechanical stirring, at room temperature. The precipitation of Fe_3O_4 magnetic powders was achieved by dropwise adding the precursor solution (50ml $FeCl_2$, 50ml $FeCl_3$) to the sodium

hydroxide solution under magnetic stirring. The Fe_3O_4 nanoparticles were then filtered and washed with distilled water until the pH reached 7. The same was done in the case of Fe_3O_4@citrate, with the mention that sodium citrate was solubilized in the NaOH solution [13].

2.2. Thick-film fabrication

The final thick films were obtained by mechanically mixing the previously obtained nanoparticles with PDMS in a 1:1 ratio, followed by ultrasonic mixing using a Hielscher UP400 ultrasonic processor. Next, the mixtures were cast, and a heat treatment at 150 °C was applied to obtain the final composite thick films. The films were further labeled as Fe_3O_4/PDMS and Fe_3O_4@Citrate/PDMS.

2.3. Physico-chemical characterization

Both types of nanoparticles were characterized to confirm the formation of single-phase magnetite by *X-ray diffraction* using a PANalytical Empyrean diffractometer with Cu radiation (Cu K=1.541874) in Bragg-Brentano geometry (Malvern PANalytical, Bruno, Netherland).

Infrared spectra were further recorded in the range 4000-400 cm^{-1}, 64 scans, at a resolution of 4 cm^{-1} using a Nicolet iS50 FT-IR spectrometer (Thermo Fisher Scientific Inc., Waltham, MA, USA) to confirm the presence of citrate in the Fe_3O_4@citrate powder. As for the membranes, FT-IR 2D maps were recorded using a Thermo Scientific Nicolet iS50R FTIR Microscope (Thermo Fisher Scientific Inc., Waltham, MA, USA), equipped with a liquid nitrogen cooled MCD detector.

The morphology of the obtained nanoparticles was investigated using a *high-resolution electron microscope* (SEM) equipped with a field emission source (FEI Inspect F50, Eindhoven, Netherlands) at 30 kV.

Magnetic properties were determined for both nanoparticles and thick-films at room temperature using a *vibrating sample magnetometer*, VSM-7400 LakeShore (Westerville, OH, USA), recording the mass magnetization at a field intensity between -10 kOe and 10 kOe.

Thermogravimetric analysis, combined with differential scanning calorimetry, was performed using a STA TG/DSC Netzsch Jupiter equipment (Selb, Germany), with the temperature ranging between 25 and 900 ºC in a dynamic atmosphere of 50 mL/min air with a heating rate of 10 K/min in an Al_2O_3 crucible.

3. Results and discussions

3.1. Analysis of magnetic powders

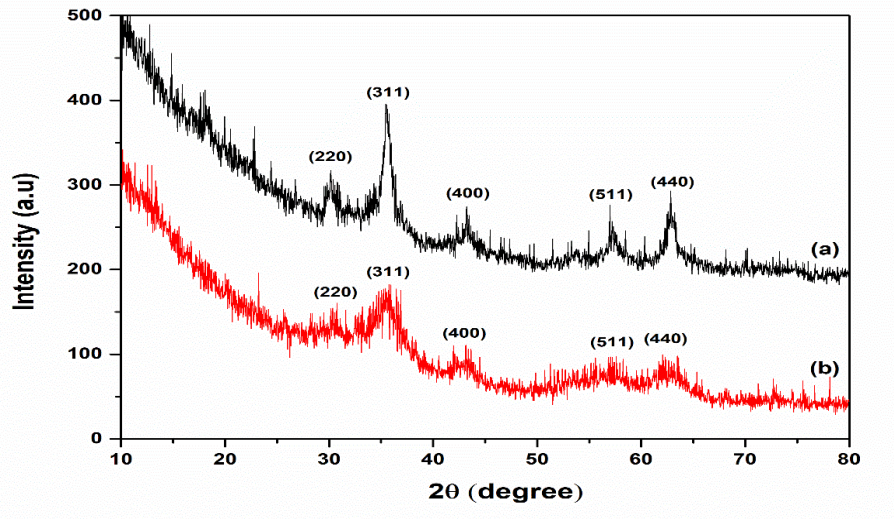

Fig. 1 X-ray diffraction patterns of synthesized Fe_3O_4 (a) and Fe_3O_4@Citrate (b)

As we can see in Fig. 1, the diffraction pattern of F_3O_4 shows six peaks around 2θ = 30, 35, 43, 54, 57, and 63 degrees that correspond to (220), (311), (400), (422), and (511) diffraction planes. According to PDF 96-900-5840, these diffraction planes are representative of cubic F_3O_4 [14]. Although sodium citrate produces a high decrease in intensity for the peaks corresponding to each of the identified planes, the overall crystalline structure of F_3O_4 is not affected by the surface modification/stabilization with citrate [14].

As shown in Fig. 2, both Fe_3O_4 and Fe_3O_4@citrate spectra showed the adsorption band at 550 cm^{-1}, characteristic of the Fe-O bond [15], as well as the 3336 cm^{-1} corresponding to -OH bonds present on the surface of the nanoparticles. By comparing the two spectra, we can clearly distinguish the appearance of additional peaks at approximately 1586 cm^{-1} and 1348 cm^{-1}, which correspond to asymmetrical and symmetrical stretching vibrations of the COO^- functional group present in the citrate molecule and may indicate the surface adsorption of the citrate onto the Fe_3O_4 nanoparticles [14].

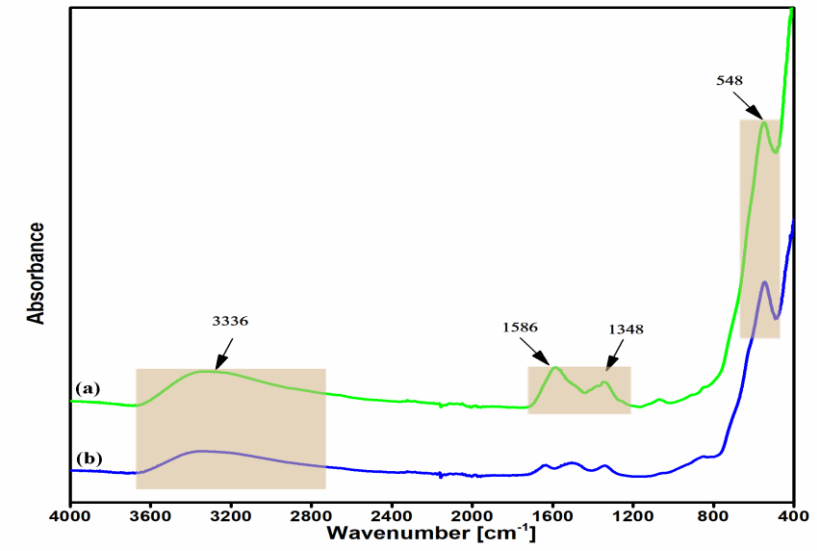

Fig. 2 FT-IR spectra of coated Fe_3O_4 (a) and uncoated Fe_3O_4 (b)

As it can be seen in Fig. 3, the absence of the hysteresis loops indicates the superparamagnetic behavior of the obtained nanoparticles [16]. The saturation magnetization of Fe_3O_4 was significantly lower compared with other studies where other synthesis methods have been employed [17,18]. Saturation magnetization (M_s) was around 35 emu/g for simple Fe_3O_4 and decreased up to 17 emu/g in the case of Fe_3O_4@Citrate (see Fig. 3). However, M_s is relatively higher when compared to others [19] and could be attributed to the very small particle size [20]. It is noteworthy that the M_s is efficient enough for removing the magnetic nanoparticles from an aqueous solution, using a strong magnet. This fact is also stated by Mohanan *et al.* [21]. The two-fold decrease in saturation magnetization is specific to coated magnetic particles [22,23].

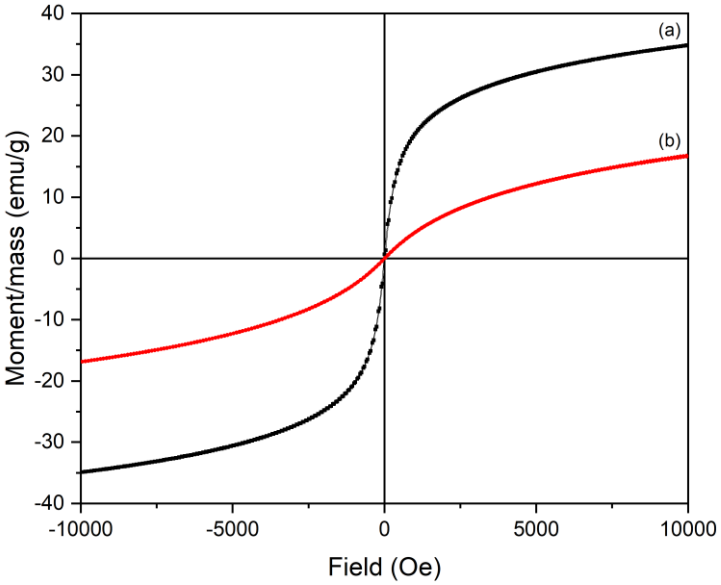

Fig. 3 Magnetic properties of Fe_3O_4 (a) and Fe_3O_4@citrate (b)

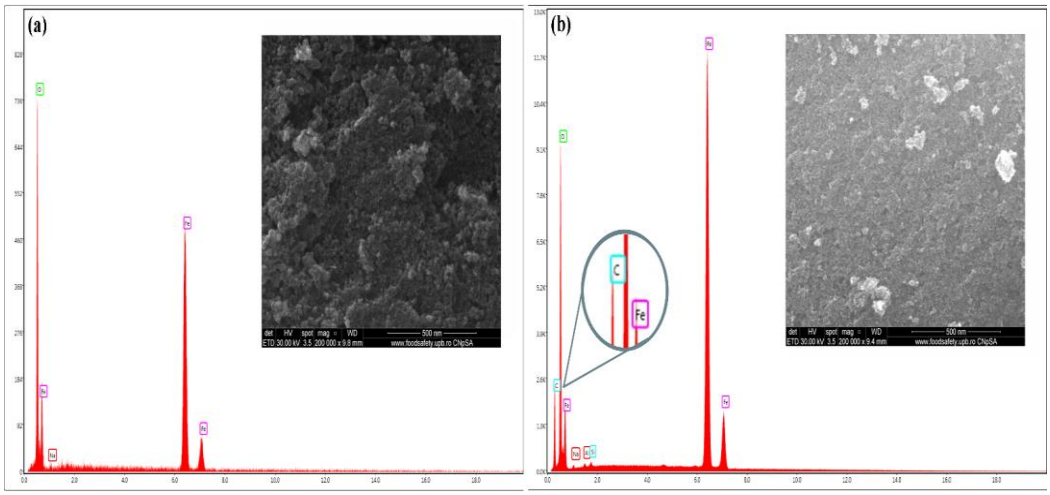

Fig. 4 Representative SEM images and EDX analysis of the Fe_3O_4 (a) and Fe_3O_4@citrate (b)

The obtained magnetite nanopowders were further subjected to SEM analysis. As shown in Fig. 4, both Fe_3O_4 and Fe_3O_4@citrate present relatively spherical particles with diameters of less than 10 nm that possess a tendency to agglomerate, probably due to magnetic dipole moment interaction between particles. As it can be seen in the insert from b, surface modification of Fe_3O_4 does not lead to any changes regarding particle size, although the coating clearly reduces the agglomeration tendency. Also, EDX analysis was performed and by comparing the two materials, in Fig. 4b we see additional elements present on the

surface, including carbon, due to the presence of the organic coating. This data supports the FTIR analysis and confirms the magnetite nanoparticles had been successfully coated with citrate anion.

3.2. Thick-film analysis

The resultant homogenous, dark brown films were measured using a digital caliper. The thickness of the obtained films was 703±14 μm for Fe_3O_4/PDMS and 709±19 μm for Fe_3O_4@Citrate/PDMS film. Measurements are given as the average value of three determinations in different areas of the film. To determine the homogeneity of the obtained films, the samples were characterized by FT-IR spectroscopy and microscopy. In the first phase, the films were analyzed using FTIR-ATR spectroscopy (Fig. 5A) to identify the chemical groups characteristic of Fe_3O_4/PDMS and Fe_3O_4@Citrate/PDMS films.

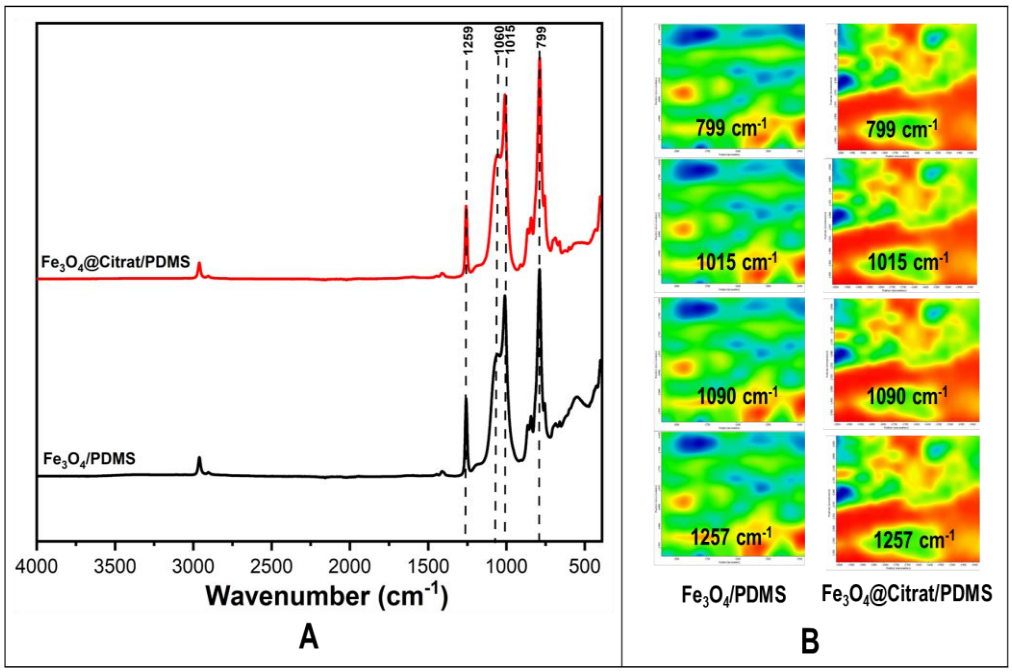

Fig. 5 FT-IR spectra (A) and FT-IR 2D maps (B) of the two magnetic films

Both films showed absorption bands characteristic of PDMS: 799 cm^{-1}, band characteristic of deformation vibrations of -CH_3 in the Si-CH_3 bond, 1015 cm^{-1}, 1060 cm^{-1} characteristic of Si-O-Si stretching and 2950 cm^{-1} characteristic of the asymmetric stretching vibrations of the CH_3- group in Si-CH_3 [c]. Starting from the FT-IR spectrum, the 799, 1015, 1090 and 1257 cm^{-1} bands were subsequently chosen to determine their distribution in the composite material, thus analyzing the homogeneity of the films. In Fig. 5B we obtained FT-IR maps

associated with the selected bands and based on the colorimetric distribution of the intensity of the characteristic bands in conjunction with the mapping of the films by SEM/EDAX analysis (Fig. 6) it can be confirmed that morphologically and compositionally homogeneous films were obtained. Additionally, elemental mapping of the membranes showed a slightly better distribution for Fe in the samples containing Fe_3O_4@citrate which is normal considering the anti-agglomerating capacity of the citrate groups (negatively charged groups). Overall, the magnetic nanopowders are uniformly distributed in the polymeric mass, successfully fulfilling the requirement for obtaining a uniform composite material.

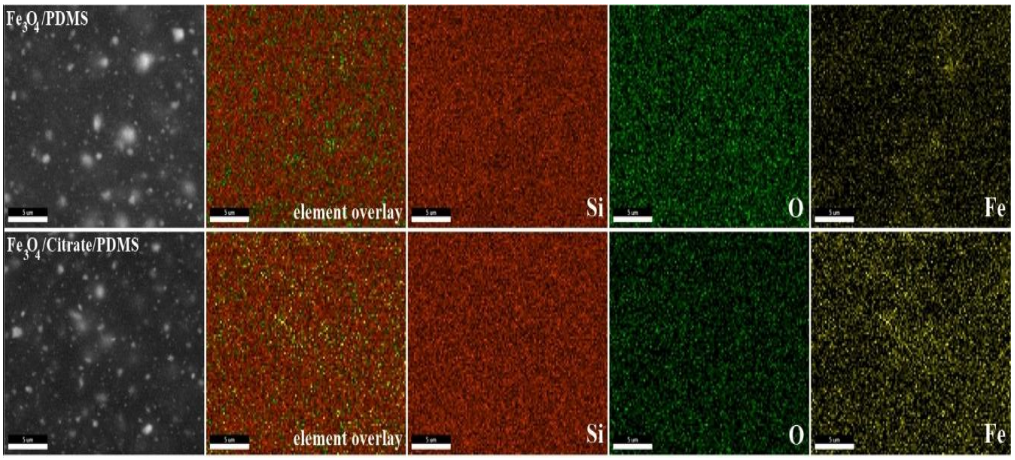

Fig. 6 SEM images and elemental mapping of nanocomposite films of Fe_3O_4/PDMS (up) and Fe_3O_4@citrate/PDMS (down)

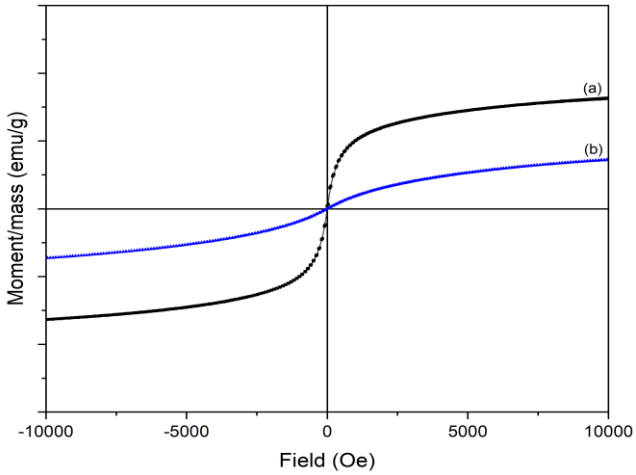

Fig. 7 M vs. H curves of Fe_3O_4/PDMS (a) and Fe_3O_4@Citrat/PDMS (b)

In terms of magnetic behavior, the trend is similar to that of magnetic powders. Specifically, Fe_3O_4@Citrate/PDMS film has a lower M_s (7.27 emu/g)

value compared to Fe_3O_4/PDMS (16.33 emu/g). Also, the films maintain their superparamagnetic behavior as no hysteresis loop is observed on the M vs. H curves. Magnetization saturation is lower compared to the powders because PDMS also acts like a coating agent after Fe_3O_4 nanoparticles were dispersed in the polymeric solution. Similar to our results, Paknahad and Tahmasebipour [8] obtained a 16.2 emu/g magnetization saturation for 25% Fe_3O_4 nanoparticles embedded in polymeric matrix. Our value is not far from theirs even though we had a 50% (wt.) Fe_3O_4. The uncoated magnetite has by far the best values when it comes to magnetic properties, taking into consideration that a 10 emu/g magnetic saturation would be suitable for targeted drug delivery systems [23].

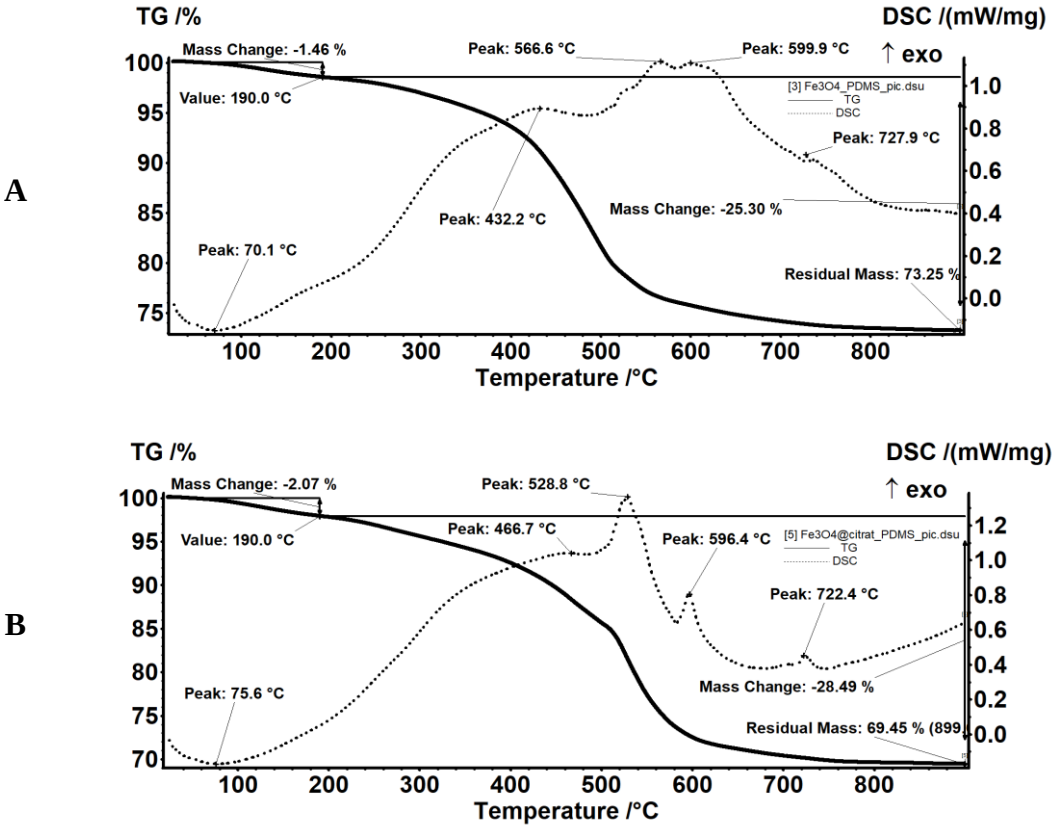

Fig. 8 TGA curves of A. Fe_3O_4/PDMS and B. Fe_3O_4@citrate/PDMS

Fe_3O_4/PDMS and Fe_3O_4@citrate/PDMS films are losing 1.46% and 0.73% of their initial masses up to 190 °C, by elimination of volatile molecules. These mass losses are characterized by an endothermic process, with minimum values at 70.1 °C and 75.6 °C for Fe_3O_4/PDMS and Fe_3O_4@citrate/PDMS, respectively. After 190 °C the samples continue to lose mass continuously, the process being more intense in 400-500 °C interval. The DSC curves indicate the presence of multiple,

overlapped exothermic processes. The polydimethylsiloxane is degraded, with formation of a SiO_2 in which the magnetic iron oxide nanoparticles will remain embedded [24,25]. Also, it is worth mentioning that the residual bit retains the magnetic properties, as it can be suspended by a normal magnet. Mass loss for each temperature range is summarized in Table 1.

Table 1.

Mass loss according to TG-DSC curves

Sample	Mass loss (%)		
	25-170°C	170-900°C	Residual mass (%)
Fe_3O_4/PDMS	1.46	25.30	73.25
Fe_3O_4@citrate/PDMS	2.07	28.49	69.45

5. Conclusions

Drawing a line on the results obtained, the study aimed to evaluate the material characteristics of a magnetic film based on PDMS and Fe_3O_4, and citrate-coated Fe_3O_4, respectively. The results are promising regarding the use of these films as an integral component of some micropumps, with great application potential in the category of BioMEMS drug delivery devices. Experimentally, two films were obtained using bare magnetite and citrate coated magnetite. The homogeneity of the films was very good in the case of both samples. Coating the magnetite in the synthesis phase improves their stability and certainly implies a much better distribution of the nanoparticles when they are incorporated into a polymer. However, we noticed that the uncoated magnetite managed to rise to the same level as the citrate-coated one in terms of the homogeneity study. This is due to the fact that PDMS ends up acting as a coating agent. The step of embedding magnetic nanoparticles in the polymer matrix is similar to the synthesis processes where magnetite is coated after the initial synthesis step (ex-situ coating method).

Acknowledgement:

This work was supported by a grant of the Romanian Ministry of Research and Innovation, CCCDI – UEFISCDI, project number PN-III-P2-2.1-PED-2019-4813, contract 522PED/2020, within PNCDI III.

R E F E R E N C E S

[1]. *F. Amirouche,Y. Zhou,T. Johnson*, "Current micropump technologies and their biomedical applications", Microsystem Technologies, **vol.15**, (5), 2009, pp.647-666.

[2]. *F. Abhari,H. Jaafar,N. Md Yunus*, "A Comprehensive Study of Micropumps Technologies", International Journal of Electrochemical Science, **vol.7**, (2012, pp.9765-9780.

[3]. *K.F. Lei*, "Microfluidic Systems for Diagnostic Applications: A Review", SLAS Technology, **vol.17**, (5), 2012, pp.330-347.
[4]. *J. Yunas,B. Mulyanti,I. Hamidah,M. Mohd Said,R.E. Pawinanto,W.A. Wan Ali,A. Subandi,A.A. Hamzah,R. Latif,B. Yeop Majlis*, "Polymer-Based MEMS Electromagnetic Actuator for Biomedical Application: A Review", Polymers, **vol.12**, (5), 2020.
[5]. *N.A. Hamid,B.Y. Majlis,J. Yunas,A.R. Syafeeza,Y.C. Wong,M. Ibrahim*, "A stack bonded thermo-pneumatic micro-pump utilizing polyimide based actuator membrane for biomedical applications", Microsystem Technologies, **vol.23**, (9), 2017, pp.4037-4043.
[6]. *R. Pawinanto,J. Yunas,A. Alwani,N. Asmantowi,S. Alva*, "Electromagnetic Micro-Actuator with Silicon Membrane for Fluids Pump in Drug Delivery System", International Journal of Mechanical Engineering and Robotics Research, **vol.**, (2019.
[7]. *C. Qi,D. Han,T. Shinshi*, "A MEMS-based electromagnetic membrane actuator utilizing bonded magnets with large displacement", Sensors and Actuators A: Physical, **vol.330**, (2021, pp.112834.
[8]. *A.A. Paknahad,M. Tahmasebipour*, "An electromagnetic micro-actuator with PDMS-Fe3O4 nanocomposite magnetic membrane", Microelectronic Engineering, **vol.216**, (2019, pp.111031.
[9]. *S. Majidi,F. Zeinali Sehrig,S.M. Farkhani,M. Soleymani Goloujeh,A. Akbarzadeh*, "Current methods for synthesis of magnetic nanoparticles", Artificial Cells, Nanomedicine, and Biotechnology, **vol.44**, (2), 2016, pp.722-734.
[10]. *M. Faraji,Y. Yamini,M. Rezaee*, "Magnetic nanoparticles: Synthesis, stabilization, functionalization, characterization, and applications", Journal of the Iranian Chemical Society, **vol.7**, (1), 2010, pp.1-37.
[11]. J. Alonso,J.M. Barandiarán,L. Fernández Barquín,A. García-Arribas. Chapter 1 - Magnetic Nanoparticles, Synthesis, Properties, and Applications. In *Magnetic Nanostructured Materials*, El-Gendy, A.A., Barandiarán, J.M., Hadimani, R.L., Eds.; Elsevier: 2018; pp. 1-40.
[12]. *L. Xiao,J. Li,D.F. Brougham,E.K. Fox,N. Feliu,A. Bushmelev,A. Schmidt,N. Mertens,F. Kiessling,M. Valldor,B. Fadeel,S. Mathur*, "Water-Soluble Superparamagnetic Magnetite Nanoparticles with Biocompatible Coating for Enhanced Magnetic Resonance Imaging", ACS Nano, **vol.5**, (8), 2011, pp.6315-6324.
[13]. *D. Ficai,E. Andronescu,A. Ficai,G. Voicu,B. Vasile,V. Ionita,C. Guran*, "Synthesis and Characterization of Mesoporous Magnetite Based Nanoparticles", CURRENT NANOSCIENCE, **vol.8**, (2012, pp.875-879.
[14]. *Y. Wei,B. Han,X. Hu,Y. Lin,X. Wang,X. Deng*, "Synthesis of Fe3O4 Nanoparticles and their Magnetic Properties", Procedia Engineering, **vol.27**, (2012, pp.632-637.
[15]. *I.L. Ardelean,L.B.N. Stoencea,D. Ficai,A. Ficai,R. Trusca,B.S. Vasile,G. Nechifor,E. Andronescu*, "Development of Stabilized Magnetite Nanoparticles for Medical Applications", Journal of Nanomaterials, **vol.2017**, (2017, pp.6514659.
[16]. *M. Abboud,S. Youssef,J. Podlecki,R. Habchi,G. Germanos,A. Foucaran*, "Superparamagnetic Fe3O4 nanoparticles, synthesis and surface modification", Materials Science in Semiconductor Processing, **vol.39**, (2015, pp.641-648.
[17]. *M.H.R. Farimani,N. Shahtahmasebi,M. Rezaee Roknabadi,N. Ghows,A. Kazemi*, "Study of structural and magnetic properties of superparamagnetic Fe3O4/SiO2 core–shell nanocomposites synthesized with hydrophilic citrate-modified Fe3O4 seeds via a sol–gel approach", Physica E: Low-dimensional Systems and Nanostructures, **vol.53**, (2013, pp.207-216.
[18]. *H. Zhang,G. Zhu*, "One-step hydrothermal synthesis of magnetic Fe3O4 nanoparticles immobilized on polyamide fabric", Applied Surface Science, **vol.258**, (11), 2012, pp.4952-4959.

[19]. *Munasir,R.P. Kusumawati*, "Synthesis and Characterization of Fe3O4@rGO Composite with Wet-Mixing (ex-situ) Process", Journal of Physics: Conference Series, **vol.1171**, (2019, pp.012048.

[20]. *T. Bui,S. Ton,A. Duong,T. Thai Hoa*, "Dependence of magnetic responsiveness on particle size of magnetite nanoparticles synthesised by co-precipitation method and solvothermal method", Journal of Science: Advanced Materials and Devices, **vol.3**, (2017.

[21]. *P.V. Mohanan,G. Geetha*, "Surface Modification of Magnetite Nanoparticles Lift up the Thermal Stability and Furnishes Superparamagnetism for Poly Meta-Amiphenol Magnetite Nanocomposites", Nanoscience & Technology: Open Access, **vol.5**, (2018, pp.1-7.

[22]. *C.Y. Gao,S. Piao*, "Pickering emulsion polymerized magnetite-poly(methyl methacrylate) composite particles and their magnetorheology", Colloid and Polymer Science, **vol.295**, (2017, pp.1-8.

[23]. *V. Ene,I. Neacsu,O. Oprea,V.-A. Surdu,R. Trusca,A. Ficai,E. Andronescu*, "Single Step Synthesis of Glutamic/tartaric Acid-stabilised Fe3O4 Nanoparticles for Targeted Delivery Systems", Revista de Chimie, **vol.71**, (2020, pp.230-238.

[24]. *C. Chircov,M.-F. Matei,I.A. Neacșu,B.Ș. Vasile,O.C. Oprea,A.M. Croitoru,R.D. Trușcă,E. Andronescu,I. Sorescu,F. Bărbuceanu*, "Iron Oxide–Silica Core–Shell Nanoparticles Functionalized with Essential Oils for Antimicrobial Therapies", Antibiotics, **vol.10**, (9), 2021, pp.1138.

[25]. *D. Istrati,A. Moroșan,R. Stan,B.Ș. Vasile,G. Vasilievici,O. Oprea,G. Dolete,B. Purcăreanu,D.E. Mihaiescu*, "Microwave-Assisted Sol-Gel Preparation of the Nanostructured Magnetic System for Solid-Phase Synthesis", Nanomaterials, **vol.11**, (12), 2021, pp.3176.